Archives of Environmental Contamination and Toxicology (2024) 86:140–151
https://doi.org/10.1007/s00244-024-01053-1

Contribution of Mine-Derived Airborne Particulate Matter to Ca, Fe, Mn and S Content and Distribution in the Lichen *Punctelia hypoleucites* Transplanted to Bajo de la Alumbrera Mine, Catamarca (Argentina)

Juan Martín Hernández[1] · Emmanuel Marie de la Fournière[2] · Cinthia Paula Ramos[2,3] · Mario Ernesto Debray[2] · Rita Rosa Plá[4] · Raquel Clara Jasan[4] · Rodrigo Invernizzi[4] · Luis Germán Rodríguez Brizuela[5] · Martha Susana Cañas[1]

Received: 29 June 2023 / Accepted: 9 January 2024 / Published online: 7 February 2024

Abstract

The aim of this work was to relate the contribution of mine-derived airborne particulate matter to Ca, Fe, Mn and S content and distribution in *Punctelia hypoleucites* transplanted to Bajo de la Alumbrera, an important open-pit mine in Catamarca, Argentina. Lichen samples were transplanted to four monitoring sites: two sites inside the mine perimeter and two sites outside the mine. After three months, elemental distribution in samples was analyzed by microparticle-induced X-ray emission (microPIXE), and elemental concentration was determined by specific techniques: Ca and Fe by instrumental neutron activation analysis, Mn by inductively coupled plasma atomic emission spectrometry and S by a turbidimetric method. A differential distribution of S and Ca in thalli transplanted in-mine sites was detected compared to that of samples transplanted outside-mine sites. An overlap of Fe and S in the upper cortex of the apothecium section was observed, leading to infer a mineral association of both elements. Similar association was observed for Ca and S. In addition to these results, the significantly higher concentration detected for S and Mn in in-mine site samples suggests a contribution of Fe, S, Ca and Mn of mining origin to the content and distribution of these elements in *P. hypoleucites*. MicroPIXE complemented with Mössbauer spectroscopy analysis determined the presence of pyrite particles together with other iron-bearing minerals displaying different degrees of oxidation. These results point to a mining origin of the airborne particulate matter trapped by the lichen thalli transplanted to Bajo de la Alumbrera. These findings indicate that *P. Hypoleucites* acts as an excellent air quality biomonitor in the Bajo de la Alumbrera mine area.

Open-pit mining impacts air quality, mainly through the emission of particulate matter. This fact is due to the extraction process itself, as well as crushing, grinding and the existence of deposits of sterile waste, among other associated activities. This extractive method involves the removal of a large amount of rock materials, which can possibly be dispersed in an area beyond the mine.

Pollution generated in the mining process has detrimental consequences on ecosystems, due not only to the physical effect that atmospheric particles can produce, but also to their chemical composition. Particles from metalliferous

✉ Juan Martín Hernández
juanhernandez@tecno.unca.edu.ar

1 Facultad de Tecnología y Ciencias Aplicadas, Universidad Nacional de Catamarca (UNCA); Centro Regional de Energía y Ambiente para el Desarrollo Sustentable – CREAS (CONICET–UNCA), Maximio Victoria 55, 4700 San Fernando del Valle de Catamarca, Catamarca, Argentina

2 Gerencia Investigación y Aplicaciones, Centro Atómico Constituyentes, Comisión Nacional de Energía Atómica, Av. Gral.Paz 1499, 1650 San Martín, Buenos Aires, Argentina

3 Instituto de Nanociencia y Nanotecnología (CNEA - CONICET), Nodo Constituyentes, Av. Gral.Paz 1499, 1650 San Martín, Buenos Aires, Argentina

4 Departamento Química Nuclear, GAANS, Centro Atómico Ezeiza, Comisión Nacional de Energía Atómica, Presbítero Juan González y Aragón Nº 15, B1802AYA Buenos Aires, Partido de Ezeiza, Argentina

5 Laboratorio de Control Químico de Procesos, Facultad de Tecnología y Ciencias Aplicadas, Universidad Nacional de Catamarca, Maximio Victoria 55, 4700 San Fernando del Valle de Catamarca, Argentina

mining can contain sulfides, heavy metals, metalloids and other chemical species which provoke adverse effects on organisms and the environment as a whole (Odumo et al. 2018).

Bajo de la Alumbrera, one of the most important open-pit mines in Argentina, is located in the central west of the province of Catamarca. As part of the environmental controls for this mining project, atmospheric particulate matter monitoring is carried out at a limited number of fixed stations outside and inside its area. However, data about sites further away from the mine, that are potentially affected by pollution, is a key issue. Obtaining this kind of information requires the simultaneous placement of a large number of sampling stations even in remote areas, which is difficult due to economic and technical reasons (Cañas et al. 2017).

An alternative to traditional air quality monitoring methods, with low cost and relatively fast implementation and execution, is the use of lichens. These organisms can be used as accumulative biomonitors due to their ability to absorb and/or retain various elements from the atmosphere, combined with their longevity and resistance to environmental stress (Loppi and Bonini 2000; Garty 2001).

A lichen is a self-sustaining ecosystem formed by the interaction of an exhabitant fungus and an extracellular arrangement of one or more photosynthetic partners and an indeterminate number of other microscopic organisms (Hawksworth and Grube 2020). Photobionts can be blue-green cyanobacteria and/or unicellular green algae. The most common mycobionts are ascomycetes. Lichen thalli are emergent systems that generate a great variety of vegetative structures, growth forms, reproduction and special biotypes (Barreno 2004). On the basis of their overall habit, lichens are traditionally divided into three main morphological groups: these are crustose, foliose and fruticose types (Büdel and Scheidegger 2008).

Foliose lichens are leaf-like, flat and only partially attached to a substrate. Foliose thalli are either homoiomerous (gelatinous lichens) or heteromerous. Typically, they have a dorsiventral organization with distinct upper and lower surfaces. Often the thallus is divided into lobes. Foliose lichens develop a great range of thallus size and diversity. The majority of lichens grow internally stratified thalli. The main subdivisions in foliose lichens are upper cortex, photobiont layer, medulla and lower cortex (Fig. 1).

As occurs in most fungi, the vast majority of lichenized ascomycetes have sexual reproduction structures called apothecia. The apothecia are open, cup-shaped or disk-shaped with the hymenium exposed to the outside and with epithecium (Barreno and Pérez-Ortega 2003).

Different mechanisms can explain the accumulation of pollutants in the lichen thallus including particle deposition onto the lichen surface or entrapment in the interhyphal spaces of the medulla, extracellular binding of cations and intracellular uptake (Garty et al. 1979; Bargagli and Mikhailova 2002; Bačkor and Loppi 2009). The entrapment of metal-containing particles has been analyzed in detail by Garty (2001), while the origin and mode of interception and

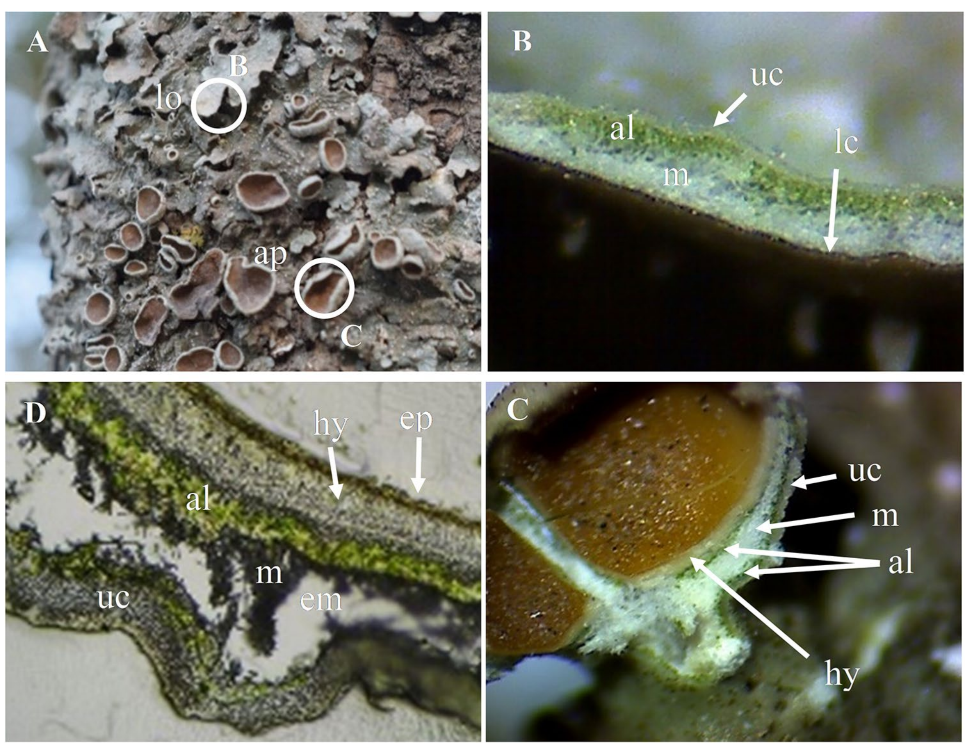

Fig. 1 **A** *Punctelia hypoleucites* thallus, *lo* Thallus lobe, *ap* Apothecium, **B** Thallus lobe perpendicular section, **C** Apothecium perpendicular section, **D** Microscopy image of the apothecium perpendicular section. The different parts of the thallus are marked by arrows and letters. Such structures are divided in these layers. *uc* Upper cortex, *al* Layer containing the photobiont (in this case alga), *m* Medulla/loosely packed hyphae, *lc* Lower cortex, *ep* Epimenium, *hy* Hymenium, *em* Empty space

incorporation of particulate matter have been reviewed by Garty and Garty-Spitz (2015).

Several analytical techniques have been used to determine the distribution and concentration of elements in the lichen thallus (Garty et al. 1979; Conti and Tudino 2016). According to Budka et al. (2004), elemental microanalysis allows more accurate air pollution studies compared to bulk (macro) analysis. In this sense, microPIXE (particle-induced X-ray emission with a scanning microprobe) allows simultaneous 2D mapping of main, minor and trace elements ($Z > 11$) of a sample with micrometric precision, providing a quantitative determination of trace elements concentration with high sensitivity (μg g^{-1} range).

Although it is possible to obtain information on the multi-elemental content of a sample by microPIXE, techniques such as INAA and ICP-OES are more appropriate for determining the total content of certain elements when the sample is a complex matrix, such as a biological tissue or a lichen thallus. According to Nečemer et al. (2008), the advantages of the INAA results are their independence from matrix effects and from sample inhomogeneities, due to the rather large effective sample mass from which the information about the elemental content is obtained. ICP-OES is more suitable for the determination when the element concentrations are below the limits of detection for INAA (Ebrahim et al. 2017). Thus, both INAA and ICP-OES allow to obtain a representative value of the elemental content of a lichen sample when it consists of several thalli conveniently crushed and homogenized for analytical purposes.

In mining areas, lichens have been used as passive biomonitors, i.e., as analyzers of the elemental accumulation in specimens in situ (Balabanova et al. 2009, 2012; Saunier et al. 2013; Odumo et al. 2014, 2018). They have also been used as active biomonitors through the application of transplantation techniques (Demková et al. 2019, 2020). With both methodologies, lichens have proven to be useful for estimating air pollution and the impact of mining activity on air quality.

Fifteen years ago, an air quality study with transplanted lichens was conducted within the Farallón Negro Volcanic Complex and its area of influence in the western region of Catamarca (Argentina). The study included four transplant sites: Bajo de la Alumbrera Cu-Mo mine and three localities potentially affected by mining emissions. In that study, *P. austrosinense* (Zahlbr.) Hale and *Canomaculina consors* (Nyl.) Elix and Hale were used as biomonitors. Active biomonitoring using both species showed to be suitable in order to relate air quality to natural or anthropogenic factors in the monitoring sites. Also, *P. austrosinense* and *C. consors* allowed to detect air pollutants from open-pit mining and proved that active biomonitoring is an adequate methodology to determine air quality in the study area (Cañas et al. 2017).

This work was part of a research project in which the lichen *Punctelia hypoleucites* (Nyl.) Krog was evaluated as bioindicator/biomonitor of air pollution in Bajo de la Alumbrera mining project and its surroundings. Unlike *P. austrosinense* and *P. consors, P. hypoleucites* is a conspicuous species of the region and, therefore, it is better adapted to the environmental conditions of the study area.

It is expected that from the determination of Fe species present in the thalli, by means of Mössbauer spectroscopy, and the knowledge of the mineralogy of the deposit, it will be possible to trace the Fe and evaluate its mining origin. Furthermore, by microPIXE analysis, a better understanding of the distribution patterns of mineral elements in the lichen tissue will be attainable. Then, this combined information will allow interpreting the response of *P. hypoleucites* to pollutants of mining origin and thus estimating its viability of use as a biomonitor of air quality in the study area.

The analyzed elements [calcium (Ca), sulfur (S), iron (Fe) and manganese (Mn)] were chosen taking into account that they correspond to the geochemical characteristics of the Bajo la Alumbrera and Bajo el Durazno deposits (Alvarez 2017; Gutiérrez et al. 2006). Other elements were discarded since their extremely low amount in the samples did not allow a good mapping.

Ca is a major element in biological systems and its distribution map obtained by microPIXE clearly indicates the structure of the selected cross sections, that matches quite well the optical microscopy photographs, and helps localizing other analytes which are in a lower amount. Fe is relevant as an indicator of iron-bearing minerals in environmental samples; in fact, during preliminary essays, microPIXE acquisition revealed a high amount of Fe in all samples. S and Mn presence also suggest a mining origin.

In this context, the aim of this work is to establish the contribution of mine-derived airborne particulate matter to Ca, Fe, Mn and S content and distribution in the biomonitor *P. hypoleucites* transplanted to Bajo de la Alumbrera mine, Catamarca (Argentina).

Materials and Methods

Study Area

The study area is located at the Central-Western region of Catamarca Province, in the extreme North of the morphostructural unit of the Northwestern Pampean Ranges (Caminos 1979). The area is characterized by the presence of narrow valleys and wide closed intermountain depressions (bolsones), alternating with uplifted basement blocks whose western slopes are usually steeper than the eastern ones. Geologically, it consists of a Precambrian igneous-metamorphic basement, mainly covered by quaternary alluvial deposits. The climate is warm arid, prevailing winds blow from NE. Precipitations are very scarce, with only about 150 to 300 mm per year, mostly in summer (about 60–70% of the total precipitation). It is located in the Monte Phytogeographic Province in the Chaqueño Domain of the Neotropical region (Morlans 1995).

In the region, there are important gold (Au), silver (Ag), copper (Cu) and molibdenum (Mo) deposits currently in operation. There it is located the first large-scale mining operation of Argentina—Bajo de la Alumbrera. It is an open-pit Cu-Au-Mo mine, which corresponds to a porphyry-type deposit included in Farallón Negro volcanic complex (Gutiérrez et al. 2006). This mine started operating in 1997 and when this work began (2018) it was in the closure phase. In its place, a Cu-Au deposit located 4 km from Bajo de la Alumbrera, Bajo El Durazno, was in open-pit mining and it has been in operation since 2015.

The study area is sparsely populated: the main locality is Andalgalá (12,600 inhabitants), the third largest city of the province. There are also little villages such as Amanao (29 inhabitants), Los Nacimientos (215 inhabitants) and Hualfín (987 inhabitants) (INDEC 2010). The four towns are located in intermountain depressions: Amanao and Andalgalá at the North end of the Bolsón de Pipanaco, Hualfin and Los Nacimientos in the Hualfin Valley. Given their relative proximity to Bajo de la Alumbrera, these human settlements are considered environmentally vulnerable. For this reason, Hualfin was chosen as a monitoring site for this study. The map of the study area, built by the ArcGIS 10.4.1 software (ESRI 2015), is displayed in Fig. 2.

Mineralization

Bajo El Durazno deposit: Mineralization of Cu-Au and in minor proportion Ag and Mo present in the veins between the stock (andesitic porphyry) and bedrock, accompanied by quartz, calcite, magnetite, pyrite (FeS_2), chalcopyrite ($CuFeS_2$) and a minor content of sericite, chlorite, orthoclase, biotite, siderite, molybdenite, bornite, sphalerite, galena, tetrahedrite–tennantite and gold. Potassic zone: potassium feldspar-biotite, in addition to disseminated mineralization of pyrite and chalcopyrite with magnetite, hematite, bornite, sphalerite and molybdenite. Sericite-clay (or phyllic) zone: abundant sulfate minerals such as jarosite ($KFe_3^{+3}(SO_4)_2(OH)_6$), natrojarosite ($NaFe_3(SO_4)_2(OH)_6$), gypsum ($CaSO_4$), with greater dissemination and veinlets of pyrite than in the potassic zone. Propylitic zone: the minerals are not described here but in Bajo de la Alumbrera deposit the typical associations of this alteration are named (Allison 1986; Sasso 1997; Alderete 1999).

Primary mineralization of Bajo de la Alumbrera deposit: chalcopyrite + pyrite ± magnetite. Potassic zone: gold-copper, secondary biotite-potassium feldspar-magnetite-quartz ± anhydrite. Propylitic zone: epidote-chlorite-albite ± magnetite. Phyllic zone (after potassic and propylitic alterations): Sericite-pyrite-quartz (González 1975; Godeas and Segal de Svetliza 1980; Sasso 1997; Angera 1999).

Sampling Procedure

In February 2018, thalli of the lichen *Punctelia hypoleucites* (Nyl.) Krog were collected from a clean site within the Northwestern Pampean Ranges region. Remnants of bark were removed from lichen thalli and placed in nylon mesh bags (length of 150 × 100 mm, mesh pore size of 1–2 mm), about 5 gr of lichen per bag. Then, lichen bags were transplanted to four monitoring sites: two sites inside the mine perimeter close to particulate matter emission sources (E1, E8), one 25 km away from the mine (E7) and another one 70 km away from the mine outside of Farallón Negro Volcanic Complex (W) (Fig. 2). At each transplant site, three bags were exposed for three months.

Elemental Distribution Analyses by microPIXE

2D maps of Ca, Fe, Mn and S elemental concentration were obtained by microPIXE, by scanning a 50-MeV $^{16}O^{5+}$ beam over cryosectioned lichen samples, at the Tandar accelerator (CNEA-Buenos Aires-Argentina). Data acquisition and processing were performed with the OMDAQ-3(Oxford Microbeams Ltd, UK) computer code. In order to analyze the elemental distribution in lichen thalli, at least two lobes and two apothecia were separated from lichen bags and were immediately frozen by using the protocol of Llabador and Moretto (1998). A mounting medium (Cryoplast®, Biopack, Argentina) was employed to avoid ice crystals formation. Afterward, transversal cross sections of lichens (Fig. 3) were obtained using a cryomicrotome at the set temperature of − 20 °C to avoid ions migration which could alter in vivo distribution. Histological cross sections were transferred to a 4-mm ultrapure polypropylene film supported by a polycarbonate washer and then freeze-dried (Southworth-Daviesa et al. 2007). Thin samples of 10 µm thickness can easily break during handling, and then, special care was taken to only irradiate those cuts which kept cell integrity as tested by optical microscopy. Usually, the typical detection limits for most elements are in the range of 1–10 µg. g^{-1} (Stoliar et al. 2004). The irradiation with heavy ion microbeams of tens of MeV energy shows significant improvement of the detection limits when analyzing heavy elements (de la Fournière et al. 2020 and references therein).

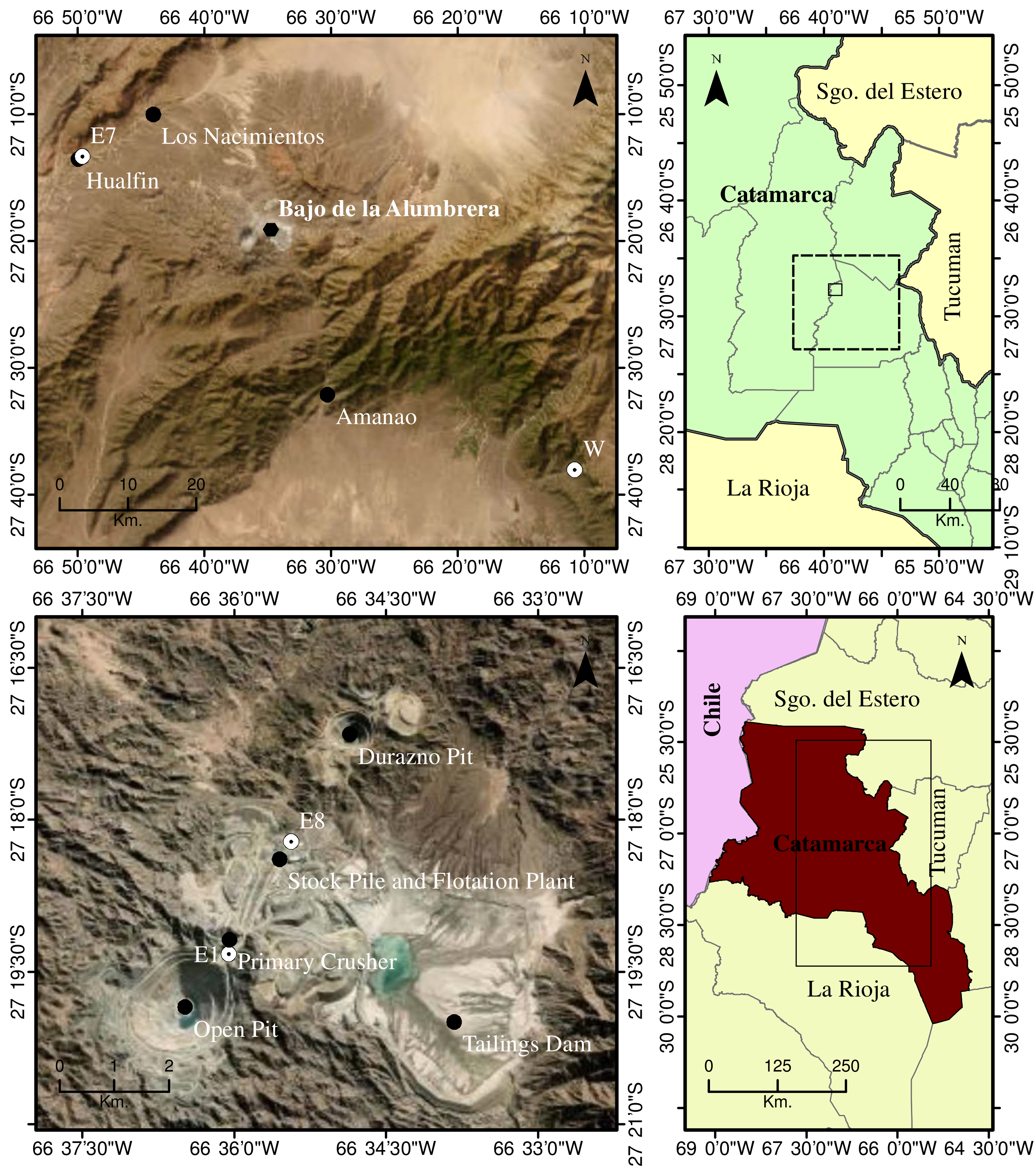

Fig. 2 **A** Map of the study area showing the outside-mine transplant sites (E7 and W). **B** Map of Bajo de la Alumbrera showing inside-mine sites (E1 and E8). The sources of particulate matter emissions from mining are also indicated (Open Pit, Durazno Pit, Tailings dam, Primary crusher, Stock pile and Flotation plant)

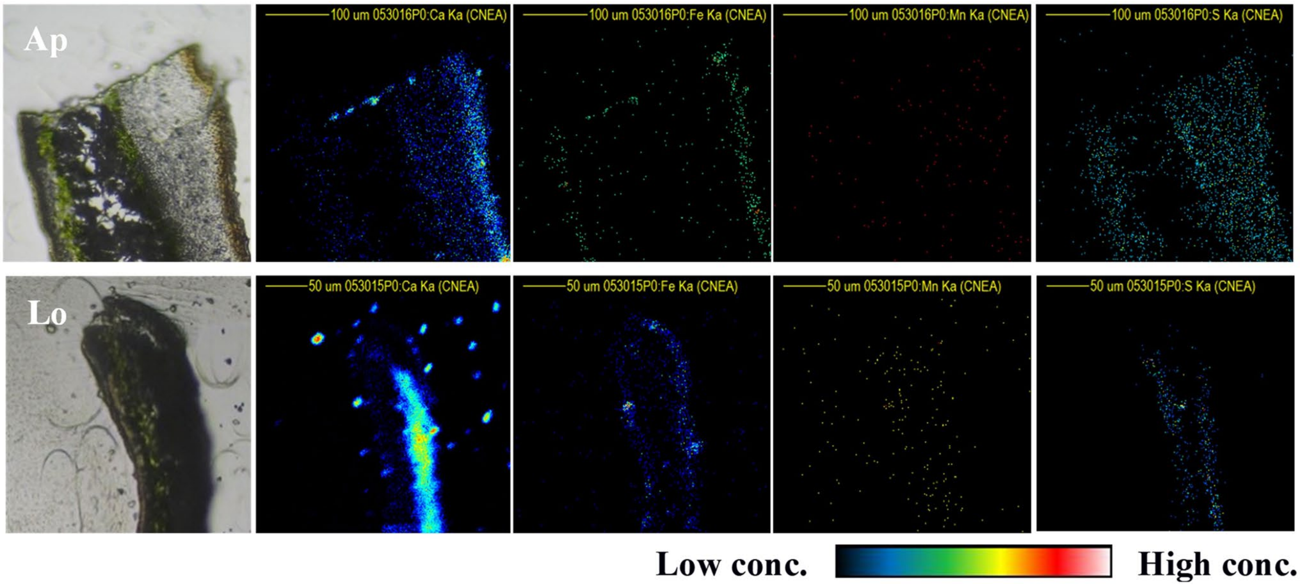

Fig. 3 Elemental distribution (Ca, Fe, Mn and S) in perpendicular section of structures that constitute this species (thallus lobe and apothecium), taken from the samples transplanted to the control site (W). Apothecium microscopy image from right to left shows epimenium, hymenium, algal layer, medulla, algal layer and upper cortex. MicroPIXE conditions: 50 MeV $^{16}O^{5+}$ beam, scan size (300 × 300–500 × 500) μm^2 (see scale bar), spot size 5 × 5μm^2. The pixels change color from blue to red with increase in elemental concentration

Table 1 Quality control results (mg kg^{-1}, dry weight) obtained for the analysis of plant WEPAL 2011-4 at the NAA laboratory

Element	Certified	Experimental
Ca	5453 ± 251	5606 ± 393
Fe	509.3 ± 39.8	526.2 ± 19.2

Analysis of Ca and Fe Content (INAA)

Instrumental neutron activation analysis (INAA) was used to determine Ca and Fe concentration (Jasan et al. 2011). Samples were ground in a Spex Centi Prep 6750 cryogenic mill and lyophilized for 24 h. About 300 mg of lyophilized material was pelletized and wrapped-up in aluminum foil for irradiation, together with two certified reference materials, NIST SRM 1633b Coal Fly Ash and IAEA Lichen 336, for calibration purposes. Irradiations were done at the RA-3 reactor (thermal flux 3.10^{13} cm^{-2} s^{-1}, 8 MW) of the Argentine National Atomic Energy Commission (Ezeiza Atomic Centre) for 4 h. Two measurements were performed after 7 and 30 day-decay using GeHP detectors (30% efficiency, 1.9 keV resolution for 1332.5 keV ^{60}Co peak), coupled to an Ortec 919E multichannel buffer module. Concentration of Ca and Fe were calculated using a non-commercial software developed at the neutron activation analysis (NAA) laboratory for internal use. Wepal 2011-4 plant was used as control sample. For all determined elements, experimental values showed good agreement with those in the material's certificate (Table 1).

Analysis of Mn Content (ICP-OES)

An accurately weighted portion of each sample (0.5 g) was placed in a porcelain crucible and ashed at 600 °C for 2 h. The ashes were digested by adding 6 ml of a 5:1 mixture of HCl (36%) and HNO_3 (65%) and heated until boiling. Then, they were filtered under vacuum to separate the solid residue. Finally, the liquid fraction was diluted to a volume of 25 ml with ultrapure water (tridistilled and deionized). Analyses for Mn were conducted with a Perkin Elmer Optima 8300 inductive plasma coupling emission spectrophotometer (ICP-OES). Metal concentrations were calculated on a dry weight basis. The precision of analysis was estimated by the relative standard deviation of three replicates and was found to be 5–10%.

Certified Reference Materials

A standard reference solution NIST SRM #3132 (Merck) was employed for the quality control of ICP-OES measurements and WEPAL 2011-4 plant was used as control sample for INAA analysis. For all determined elements, experimental values showed good agreement with those in the material's certificate.

Analysis of Sulfur Content

So as to analyze the sulfur content, a 2.5 ml of $Mg(NO_3)_2$ saturated solution was added to 0.25 g of lichen samples and dried in an electric heater. Subsequently, the sample was heated in an oven for 2 h at 500 °C. The ashes were then suspended in HCl 6 M, filtered, and the resulting solution was boiled for 3 min. The solution was brought to 25 ml with tridistilled and deionized water. The amount of SO_4^{2-} in the solution was determined by turbidimetric method with barium chloride (González and Pignata1994) which thus allowed for the calculation of sulfur content in each sample. The concentration was expressed in mg of total sulfur g^{-1} dry weight.

Statistical Analysis

One-way analysis of variance (ANOVA) was used to compare the elemental concentration of *P. hypoleucites* transplanted to the monitoring sites. Lead significance difference (LSD) Fisher's test for multiple comparisons was performed to identify sites with significantly different elemental content (*p value* < 0.05).

Iron Minerals Identification-Mössbauer Spectroscopy

Mössbauer spectroscopy was performed in the transmission mode using a ^{57}Co source in a Rh matrix. Samples for this purpose were pulverized in an agate mortar and then compacted in an acrylic holder. The spectra were collected at room temperature (RT) and then fitted with the Normos software (Brand 2010). Isomer shift (IS) values were taken relative to that of α-Fe at RT.

Results and Discussion

Elemental distribution maps corresponding to the different transplant sites show that Fe is only detected on the lichen surface, in the upper and lower cortex of thallus and epimenium of apothecium (Figs. 3, 4, 5 and 6).

Sulfur was preferentially distributed in the algal layer of lichen thallus lobe and apothecia of the off-mine and control site samples (Figs. 3, 4). A high concentration of S in the algal layer was already reported by Budka et al. (2002), Clark et al. (1999) and Paul et al. (2003). The algal layer is metabolically the most active part of the lichen thallus, producing photosynthates that are necessary for the growth of the whole lichen (Palmqvist 2000).

For the samples corresponding to the inside-mine sites (E1 and E8), S was located superficially in some sectors of the upper cortex and epimenium, in addition to the algal layer. Moreover, an overlap of S and Fe maximum concentration in the upper cortex of the apothecium section was observed, suggesting a mineralogical association of these elements (Figs. 5, 6). Mineralization at Alumbrera is abundant in S and Fe-bearing compounds such as

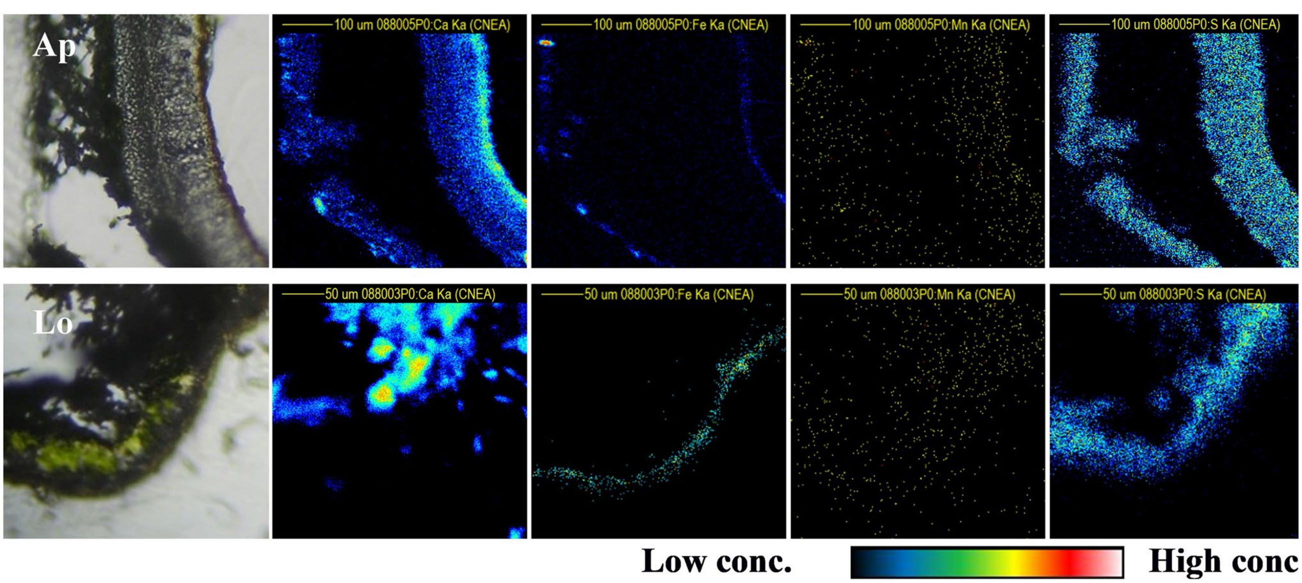

Fig. 4 Elemental distribution (Ca, Fe, Mn and S) in perpendicular section of two structures that constitute this species (thallus lobe and apothecium), taken from the samples transplanted to the outside-mine site (E7). Apothecium microscopy image from right to left shows epimenium, hymenium, algal layer, medulla, algal layer and upper cortex. Thallus lobe from bottom to top shows upper cortex, algal layer and medulla. Lower cortex is not distinguishable in this cut. Same microPIXE conditions as in Fig. 3. Scan size (300 × 300–500 × 500) μm^2 (see scale bar)

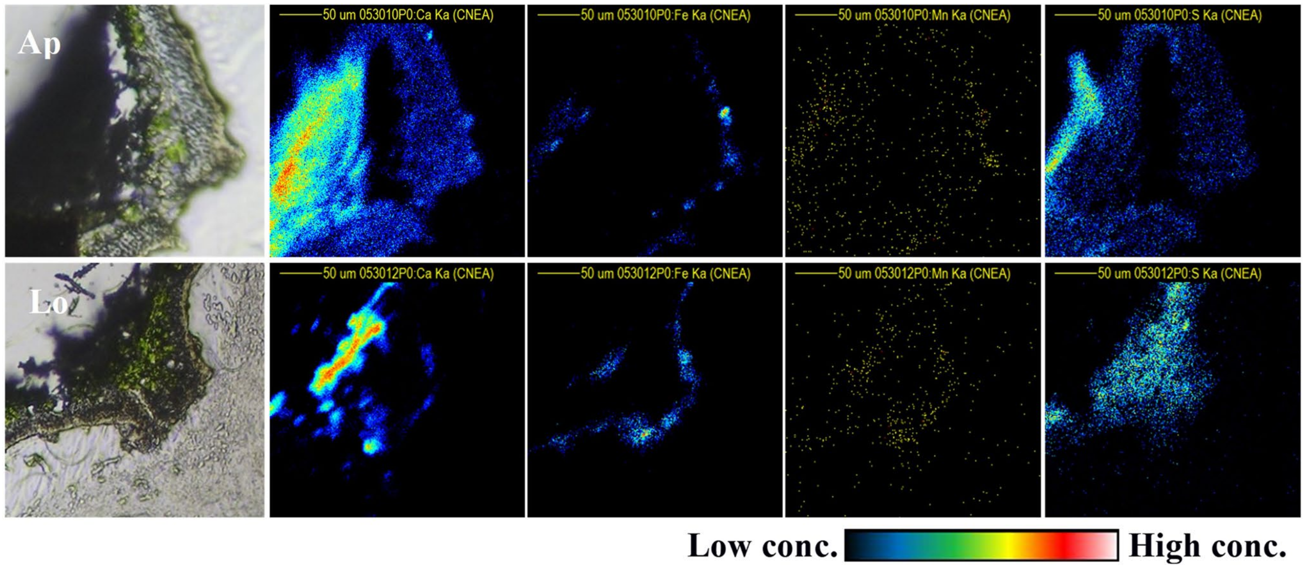

Fig. 5 Elemental distribution (Ca, Fe, Mn and S) in perpendicular section of two structures that constitute this species (thallus and apothecium), taken from the samples transplanted to the in-mine site (E1). Apothecium microscopy image from right to left shows upper cortex, algal layer, medulla. Hymenium and epithecium are not clearly distinguishable in this cut by the quality of the histological slice. Thallus lobe from bottom to top shows upper cortex, algal layer and medulla. Lower cortex is not distinguishable in this cut. Same microPIXE conditions as in Fig. 3. Scan size (300 × 300–500 × 500) μm^2 (see scale bar)

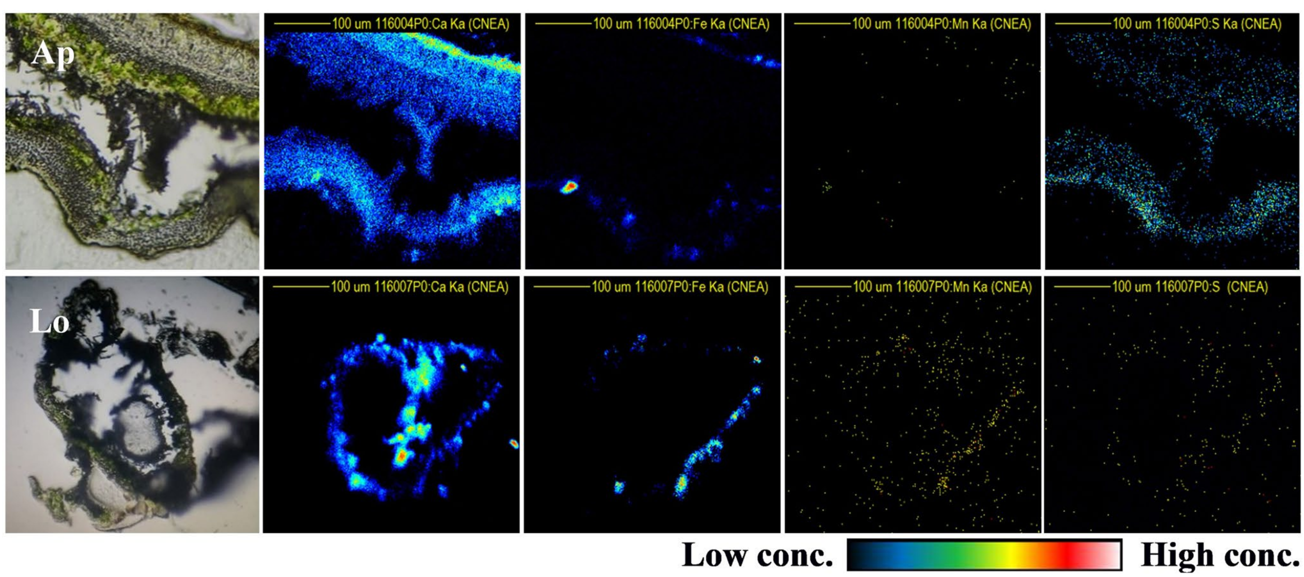

Fig. 6 Elemental distribution (Ca, Fe, Mn and S) in perpendicular section of two structures that constitute this species (thallus and apothecium), taken from samples transplanted to the in-mine site (E8). Apothecium microscopy image from bottom to top shows upper cortex, algal layer, medulla, algal layer, hymenium and epimenium. Thallus lobe from left to right shows upper cortex, algal layer and medulla. Lower cortex is not distinguishable in this cut. Same microPIXE conditions as in Fig. 3. Scan size (450 × 450) μm^2 (see scale bar)

sulfides (pyrite and chalcopyrite) and sulfates (jarosite and natrojarosite) (Sasso 1997; Alderete 1999). The higher concentrations of Fe and S detected in thalli exposed at in-mine sites (Table 2) would contribute to associate these elements with the geochemistry of the deposit thus attributing their presence to particles of mining origin trapped in the lichen structures.

At all sites, Ca is preferentially distributed in the medulla and in the epimenium (Figs. 3, 4, 5 and 6). High levels of Ca, in the form of oxalate crystal deposits, have been observed

Table 2 Elemental concentrations in lichens transplanted to inside-mine sites (E1, E8), an offside mine site (E7) and a control site (W)

Sites	Ca	Fe	Mn	S
W	49,533 ± 7292	6153 ± 463ab	77 ± 13b	1668 ± 24b
E7	53,133 ± 7427	5188 ± 97c	76 ± 6b	1416 ± 60c
E1	54,933 ± 1021	5735 ± 678bc	80 ± 4b	1954 ± 177a
E8	53,667 ± 2802	6757 ± 511a	102 ± 9a	1875 ± 165ab
ANOVA	NS	*	*	*

Values correspond to mean ± standard deviation (mg kg^{-1}, dry weight) data obtained from the whole thalli. Values followed by the same letter do not differ significantly at a $p < 0.05$ (LSD Fisher's test).

NS Nonsignificant differences

in the medulla of some lichens (Baran and Monje 2008; Modenesi et al. 2000; Paul et al. 2003), suggesting that they have a physiological function. These deposits might serve as a kind of reservoir to provide minimal but essential water levels for the photosynthetic activity of the photobiont during prolonged dry periods and generate light reflection to the algal cells, therefore helping to maximize the efficiency of photosynthesis (Clark et al. 2001).

At the inside-mine site E8, Ca was also distributed in the upper cortex, although to a lesser extent. Mineralization at Bajo El Durazno is rich in gypsum ($CaSO_4$) and calcite ($CaCO_3$) (Sasso 1997; Alderete 1999). Considering that the inside-mine sites are close to sources of particulate matter emissions from the mineralized zone, surface Ca could be associated with this source. Although the upper cortex distribution of Ca in the lichen samples transplanted to E8 could infer a mining origin, this is not observed in E1, which is also located inside the mine perimeter. Furthermore, considering that the concentration of this element did not show significant differences between sites, it is assumed that Ca of mining origin does not represent a significant contribution to the Ca content observed at all sites (Table 2).

The maps do not show a detailed Mn distribution in the lichen due to the fact that its concentration is much lower than that for the other elements. However, from the lobe maps corresponding to E1 and E8 sites and the apothecia map of E8 site, where more concentrated points can be identified in some sectors, Mn seems to have the same distribution as Fe (Figs. 3, 4, 5 and 6). It should be noted that Mn is used as a mining indicator in Minera Alumbrera Ltd environmental impact reports (Alvarez 2017) and is a representative element of Bajo el Durazno and Bajo la Alumbrera deposits (Gutiérrez et al. 2006). A significantly higher concentration of Mn was detected in lichens transplanted to the E8 site in comparison with the other transplant sites (Table 2). This result, added to the similar distribution of Mn and Fe in the thalli transplanted to inside-mine sites, would allow to infer that both elements are associated to atmospheric particles of the same origin.

The RT Mössbauer spectra for samples obtained from lichens transplanted to E1 and E8 sites (inside-mine sites) are displayed in Fig. 7. The scarce amount of sample available from lichens transplanted to E1 was detrimental to a good signal-to-noise ratio. Nevertheless, some information could be obtained from the spectrum by comparing it with that corresponding to E8 sample, with enough mass to perform the analysis.

Both spectra were fitted to three broad sextets and two quadrupole doublets. On the one hand, the sextet with hyperfine field around 51 T (S1) is characteristic of hematite while the sextet around 48 T (S2) is typical of partially oxidized magnetite, and the last one around 38 T (S3) is ascribed to a minor contribution of goethite (Murad and Johnston 1987). On the other hand, the major doublet (D1) with quadrupole splitting (QS) 0.72 mms^{-1} and IS 0.28 mms^{-1} is attributed to pyrite (FeS_2) (Stevens et al. 2005), and the other one (D2) with QS 2.30 mms^{-1} and IS 1.25 mms^{-1} is ascribed to ferrous sulfate ($FeSO_4$) (Dong et al. 2002). The scarce amount of sample available or the lack of Fe-bearing compounds, hindered the possibility of obtaining Mössbauer spectra for lichen samples transplanted to E7 and W sites.

According to the description of the mineralization detailed in the Study Area section for the Bajo el Durazno deposit, the main Fe minerals composing the deposit are sulfides (pyrite, chalcopyrite and bornite), oxides (magnetite and hematite) and sulfates (jarosite and natrojarosite) and to a lesser extent chlorite, biotite, siderite and tetrahedrite–tennantite. All Fe-bearing compounds detected in lichens by Mössbauer analysis are consistent with the minerals described for the porphyry-type deposit, with the exception of goethite. Goethite is a secondary mineral, a product of surface alteration of primary minerals such as pyrite, marcasite, arsenopyrite, chalcopyrite, siderite, magnetite and others that have been exposed to atmospheric conditions (Tabelin et al. 2020). As a result of sulfides oxidation, hydrated oxides and oxyhydroxides are formed, which give the characteristic colors (orange, reddish or brownish) to the deposits of barren material after a certain time. Therefore, the presence of goethite in lichens transplanted to inside-mine sites would indicate the incorporation into the thalli of particles from sulfides mine tailings (waste dumps, stock-piles and tailing dump) subjected to oxidative processes.

Conclusions

By means of microPIXE, a differential distribution of S and Ca could be detected in relation to that corresponding to the sample coming from the location of the transplant site. In the inside-mine sites, an overlap of Fe and S in

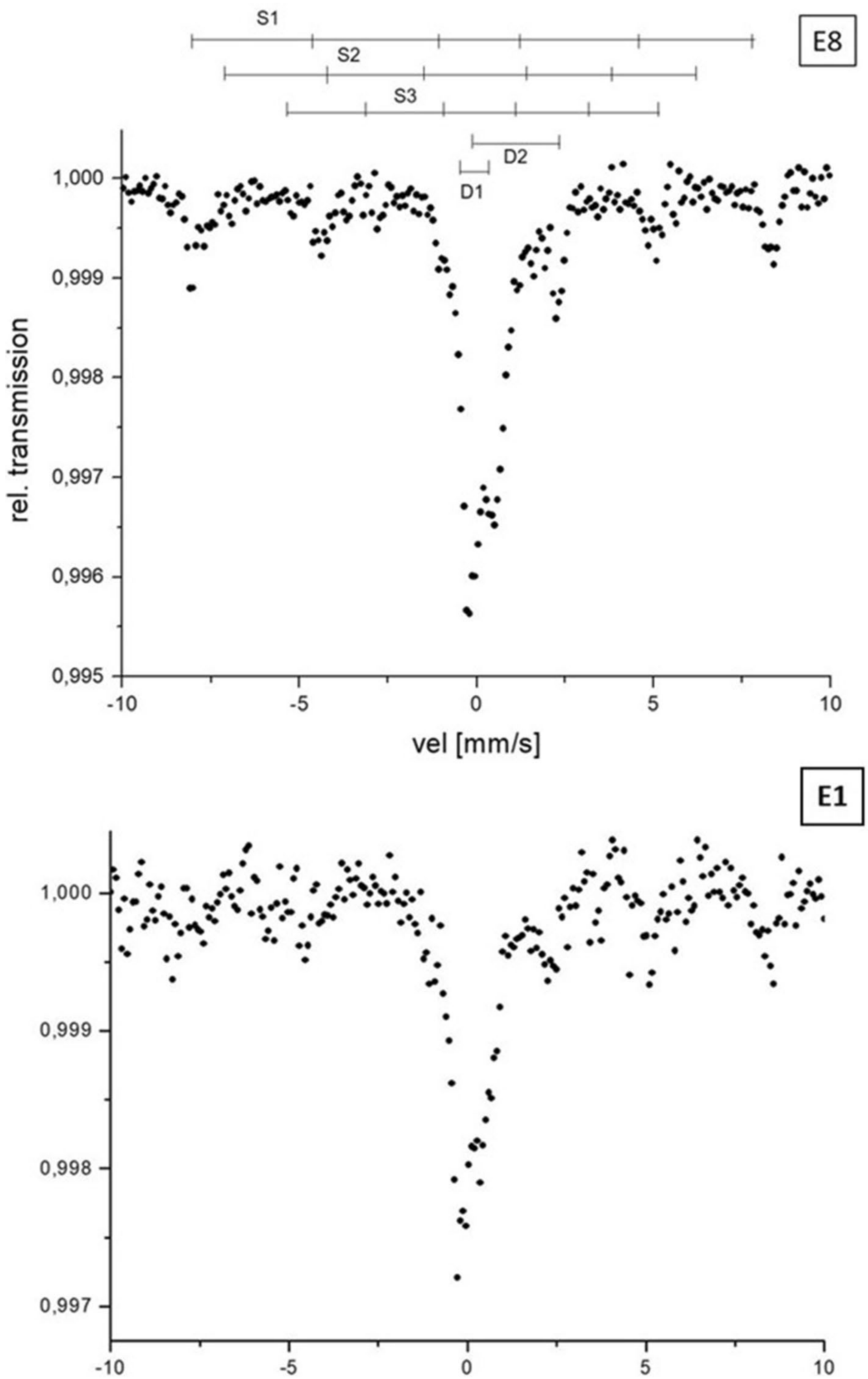

Fig. 7 Mössbauer spectra of samples E8 (upper) and E1 (lower) at RT. The corresponding subspectra were identified as S1. S2 and S3 (sextets) and D1 and D2 (doublets)

the upper cortex of the apothecium section was observed, leading to deduce a mineral association of both elements. Something similar was observed for Ca and S. These results, added to the significantly higher concentration of S and Mn detected in inside-mine site samples, allow inferring a contribution of Fe, S, Ca and Mn to the content and natural distribution of these elements in *P. hypoleucites;* then, it can be concluded that this input comes from mining-derived particulate matter in the thalli specimens transplanted to the Bajo de la Alumbrera open-pit mining project.

Sulfur and Fe distribution obtained by microPIXE complemented with Mössbauer spectroscopy analysis determined the presence of pyrite (FeS_2) and ferrous sulfate particles in the apothecia of lichens located in-mine sites. Mössbauer spectra characteristic of other iron-bearing minerals in different degrees of oxidation were also identified in the structures, in particular goethite.

These results make it possible to trace the mining origin of airborne particulate matter trapped by the lichen in the mining area and, from an analytical point of view, highlight the importance of combining complementary techniques such as microPIXE, ICP-AES, INAA and Mossbauer spectroscopy.

The information obtained from this study is valuable, as it indicates that *P. Hypoleucite*s is an excellent air quality biomonitor in the Bajo de la Alumbrera mine area.

Author Contributions JMH, MSC and EM de la F contributed to the study conception, design and data collection. Sampling and material preparation were performed by JMH. Analysis and validation of experiments were performed by JMH, EMde la F, CPR, RCJ, RRP, RI and LGRB. The first draft of the manuscript was written by JMH and MSC, and EM de la F, CPR and RRP commented on previous versions of the manuscript. All authors read and approved the final manuscript. MSC obtained financial support for this research.

Funding This work was supported by Secretariat of Science and Technology of the National University of Catamarca (RES. C.S. N° 031/18), Government secretariat for science, technology and productive innovation (RESOL-2018-70-APN-SGCTEIP#MCT) and National Council for Scientific and Technical Research (RES. D. N° 1406/14).

Data Availability The datasets generated during the current study are available from the corresponding author on reasonable request.

Declarations

Conflict of interest The authors have no relevant financial or non-financial interests to disclose.

References

Alderete M (1999) Bajo de Agua Tapada, Catamarca. Recursos Minerales de la República Argentina, Instituto de Geologıa y Recursos Minerales SEGEMAR (Buenos Aires). Anales 35:1475–1478

Allison AE (1986) The geology of the Bajo el Durazno porphyry copper-gold prospect, Catamarca province, Argentina: unpublished M. Sc (Doctoral dissertation, thesis, Tucson, AZ, University of Arizona)

Alvarez VA (2017) Determinación de niveles de referencia de calidad de aire y su relación con la geología, en áreas circundantes al complejo volcánico Farallón Negro, Provincia de Catamarca [Tesina, Facultad de Tecnología y Ciencias Aplicadas, UNCa]. Repositorio Institucional de acceso abierto, Facultad de Tecnología y Ciencias Aplicadas, UNCa

Angera JA (1999) Mina bajo de la alumbrera, Catamarca. Recursos Minerales de la República Argentina, SEGEMAR, Anales 35:1451–1461

Bačkor M, Loppi S (2009) Interactions of lichens with heavy metals. Biol Plant 53(2):214–222

Balabanova B, Stafilov T, Baceva K, Sajn R (2009) Atmospheric pollution with copper around the copper mine and flotation, Bučim, republic of Macedonia, using biomonitoring moss and lichen technique. GeologicaMacedonica 23:35–41

Balabanova B, Stafilov T, Sajn R, Baceva K (2012) Characterisation of heavy metals in lichen species hypogymniaphysodes and evernia prunastri due to biomonitoring of air pollution in the vicinity of copper mine. Int J Environ Res 6(3):779–794

Baran EJ, Monje PV (2008) Oxalate biominerals. Biominer From Nat Appl 4:219–254

Bargagli R, Mikhailova I (2002) Accumulation of inorganic contaminants. Monitoring with lichens—monitoring lichens. Springer, Dordrecht, pp 65–84

Barreno E, Pérez-Ortega S (2003) Los líquenes y el medio. Consejería del medio ambiente. ordenación del territorio e infraestructuras del Principado de Asturias. KRK ediciones

Barreno E (2004) Hongos simbiontes: líquenes, micoficobiosis y micorrizas. Botánica 309–340

Brand RA (2010) WinNormos for Igor v. http://www.wissel-gmbh.de

Büdel B, Scheidegger C (2008) Thallus morphology and anatomy. Lichen biology 40–68

Budka D, Przybyłowicz WJ, Mesjasz-Przybyłowicz J, Sawicka-Kapusta K (2002) Elemental distribution in lichens transplanted to polluted forest sites near Kraków (Poland). Nucl Instrum Methods Phys Res Sect B 189(1–4):499–505

Budka D, Mesjasz-Przybyłowicz J, Przybyłowicz WJ (2004) Environmental pollution monitoring using lichens as bioindicators: a micro-PIXE study. Radiat Phys Chem 71(3–4):783–784

Caminos R (1979) Sierras Pampeanas Noroccidentales. Salta, Tucumán, Catamarca, La Rioja y San Juan. In: Segundo simposio de geología regional Argentina academia nacional de ciencias, córdoba, Argentina 1: 225–291

Cañas MS, Jasan RC, Plá RR (2017) Lichens as bioindicators of air quality in mining areas of Latin America, with special reference to Catamarca, Argentina. In: Ecotoxicology in Latin America. Nova Science Publishers. Inc., Incorporated, 437–456

Clark BM, St. ClairMangelsonReesGrantBench LLNFLBPGGS (2001) Characterization of mycobiont adaptations in the foliose lichen *Xanthoparmelia chlorochroa* (Parmeliaceae). Am J Bot 88(10):1742–1749

Clark BM, Mangelson NF, St Clair LL et al (1999) Analysis of lichen thin sections by PIXE and STIM using a proton microprobe. Nucl Instrum Methods Phys Res Sect B 150:248–253

Conti ME, Tudino MB (2016) Lichens as biomonitors of heavy-metal pollution. Compr Anal Chem 73:117–145

de la Fournière EM, Vega NA, Müller NA, Debray ME (2020) Micro-PIXE analysis of removal of aqueous U(VI) by *S. intermedia* and *P. stratiotes* in the presence of Th (IV). Nucl Instr Meth Phys Res B 477:87–90

Demková L, Árvay J, Bobuľská L, Hauptvogl M, Michalko M (2019) Activity of the soil enzymes and moss and lichen biomonitoring method used for the evaluation of soil and air pollution from tailing pond in Nižná Slaná (Slovakia). J Environ Sci Health Part A 54(6):495–507

Demková L, Árvay J, Bobuľská L, Hauptvogl M, Michalko M, Michalková J, Jančo I (2020) Evaluation of soil and ambient air pollution around un-reclaimed mining bodies in NižnáSlaná (Slovakia) post-mining area. Toxics 8(4):96

Dong XL, Choi CJ, Kim BK (2002) Structural and magnetic characterization of Fe nanoparticles synthesized by chemical vapor condensation process. J Appl Phys 92(9):5380–5385

Ebrahim AM, Bounouira H, Abdassalam M et al (2017) Integration of instrumental neutron activation analysis and inductively coupled plasma-optical emission spectrometry with mathematical modeling for the elemental analysis of plants. Instrum Sci Technol 45(5):525–540

ESRI (2015) ArcGIS desktop: release 10.4.1. Redlands, CA

Garty J (2001) Biomonitoring atmospheric heavy metals with lichens: theory and application. Crit Rev Plant Sci 20(4):309–371

Garty J, Garty-Spitz RL (2015) Lichens and particulate matter: interrelations and biomonitoring with lichens. In: Upreti D, Divakar P, Shukla V, Bajpai R (eds) Recent advances in lichenology. Springer, New Delhi, pp 47–85

Garty J, Galun M, Kessel M (1979) Localization of heavy metals and other elements accumulated in the lichen thallus. New Phytol 82(1):159–168

Godeas MC, Segal de Svetliza SJ (1980) Alteración hidrotermal y mineralización en el Bajo la Alumbrera, Provincia de Catamarca. RevAsocGeol Argentina 35:318–331

González CM, Pignata ML (1994) The influence of air pollution on soluble proteins, chlorophyll degradation, MDA, sulphur and heavy metals in a transplanted lichen. Chem Ecol 9(2):105–113

González OE (1975) Geología y alteración en el cobre porfídico "Bajo La Alumbrera", República Argentina. In: II Congreso Ibero-Americano de Geología Económica Buenos Aires 2: 247–270

Gutiérrez AA, Chong G, Espinoza S (2006) Niveles de exposición de yacimientos del distrito minero Agua de Dionisio (YMAD), Catamarca. Revis De La Asoc Geol Argent 61(2):269–278

Hawksworth DL, Grube M (2020) Lichens redefined as complex ecosystems. New Phytol 227(5):1281

Jasan RC, Mohaded Aybar CB, Ocampo AI, Palomeque LR, Cañas MS (2011) Elemental composition analysis in lichens transplanted to the western region of Catamarca, Argentina. Int J Environ Health 5(4):304–317

Llabador Y, Moretto P (1998) Applications of nuclear microprobe in the life sciences: an efficient analytical technique for the research in biology and medicine. World Scientific, Singapore

Loppi S, Bonini I (2000) Lichens and mosses as biomonitors of trace elements in areas with thermal springs and fumarole activity (Mt. Amiata, central Italy). Chemosphere 41(9):1333–1336

Modenesi P, Piana M, Giordani P, Tafanelli A, Bartoli A (2000) Calcium oxalate and medullary architecture in *Xanthomaculinaconvoluta*. TheLichenologist 32(5):505–512

Morlans MC (1995) Regiones naturales de Catamarca. Provincias geológicas y provincias fitogeográficas. Revista de Ciencia y Técnica 2(2):1–42

Murad E, Johnston JH (1987) Iron oxides and oxyhydroxides. In: Long G. (ed) Mössbauer spectroscopy applied to inorganic chemistry. Plenum Publ. Corp, New York, 2: 507–582

INDEC (2010) Región Catamarca. https://www.indec.gob.ar/indec/web/Nivel4-CensoProvincia-3-999-10-000-2010. Accessed 26 June 2023

Nečemer M, Kump P, Ščančar J et al (2008) Application of X-ray fluorescence analytical techniques in phytoremediation and plant biology studies. SpectrochimActa Part B Atomicspectrosc 63(11):1240–1247

Odumo BO, Carbonell G, Angeyo HK, Patel JP, Torrijos M, Rodríguez Martín JA (2014) Impact of gold mining associated with mercury contamination in soil, biota sediments and tailings in Kenya. Environ Sci Pollut Res 21(21):12426–12435

Odumo BO, Nanos N, Carbonell G, Torrijos M, Patel JP, Rodríguez Martín JA (2018) Artisanal gold-mining in a rural environment: land degradation in Kenya. Land Degrad Dev 29(10):3285–3293

Palmqvist K (2000) Carbon economy in lichens. New Phytol 148(1):11–36

Paul A, Hauck M, Fritz E (2003) Effects of manganese on element distribution and structure in thalli of the epiphytic lichens Hypogymniaphysodes and Lecanoraconizaeoides. Environ Exp Bot 50(2):113–124

Sasso AM (1997) Geological evolution and metallogenetic relationships of the Farallón Negro Volcanic Complex, NW Argentina. Unpublished Ph.D. thesis, Kingston, ON, Queen`s University, 841

Saunier JB, Losfeld G, Freydier R, Grison C (2013) Trace elements biomonitoring in a historical mining district (les Malines, France). Chemosphere 93(9):2016–2023

Southworth-Daviesa RJ, Leatha K, Grime G, Garmana E (2007) The characterisation of a contaminant-free support film for micropixe analysis of biological samples. In: Proceedings of the XI international conference on PIXE and its analytical applications Puebla, Mexico 25–29

Stevens JG, Khasanov A, Miller JW, Pollak H, Li Z (2005) Mössbauer mineral handbook. Mössbauer Effect Data Center

Stoliar P, Kreiner AJ, Debray ME et al (2004) Microdistributions of prospective BNCT-compound CuTCPH in tissue sections with a heavy ion microbeam. Appl Radiat Isot 61(5):771–774

Tabelin CB, Corpuz RD, Igarashi T et al (2020) Acid mine drainage formation and arsenic mobility under strongly acidic conditions: importance of soluble phases, iron oxyhydroxides/oxides and nature of oxidation layer on pyrite. J Hazard Mater 399:122844